

---

# WHAT DO TEMPORAL GRAPH LEARNING MODELS LEARN?

---

**Abigail J. Hayes\***  
University of Mannheim  
abigail.hayes@uni-mannheim.de

**Tobias Schumacher\***  
University of Mannheim,  
RWTH Aachen University  
tobias.schumacher@uni-mannheim.de

**Markus Strohmaier**  
University of Mannheim,  
GESIS - Leibniz Institute for the Social Sciences, and  
Complexity Science Hub Vienna  
markus.strohmaier@uni-mannheim.de

## ABSTRACT

Learning on temporal graphs has become a central topic in graph representation learning, with numerous benchmarks indicating the strong performance of state-of-the-art models. However, recent work has raised concerns about the reliability of benchmark results, noting issues with commonly used evaluation protocols and the surprising competitiveness of simple heuristics. This contrast raises the question of which characteristics of the underlying graphs temporal graph learning models actually use to form their predictions. We address this by systematically evaluating eight models on their ability to capture eight fundamental characteristics related to the link structure of temporal graphs. These include structural characteristics such as density, temporal patterns such as recency, and edge formation mechanisms such as homophily. Using both synthetic and real-world datasets, we analyze how well models learn these characteristics. Our findings reveal a mixed picture: models capture some characteristics well but fail to reproduce others. With this, we expose important limitations. Overall, we believe that our results provide practical insights for the application of temporal graph learning models and motivate more interpretability-driven evaluations in graph learning research.

## 1 Introduction

Learning on temporal graphs has become an increasingly popular research topic, exemplified by the emergence of a multitude of benchmarks [e.g., 6, 10, 11], on which state-of-the-art graph learning models often appear to achieve very strong results. At the same time, the benchmark performances on link prediction tasks have faced increased scrutiny: from flaws in test sets and evaluation metrics leading to unrealistic results [4, 16, 18] to heuristics, such as predicting edges involving recently active and globally popular nodes [5], performing on par with state-of-the-art models. Further, even if specific models perform well on given benchmarks, it is not clear which factors contribute to this or, more specifically, which graph characteristics models pick up on to form their predictions.

In light of these issues with the evaluation of link prediction, we aim to step back and evaluate the ability of popular graph learning models to learn simple, interpretable characteristics of temporal graphs. Specifically, we evaluate the ability of dynamic graph learning models to learn eight different characteristics: the general graph characteristics of *temporal granularity*, *edge direction* and *density*, temporal patterns with *edge persistence*, *periodicity* and *recency*, and edge formation mechanisms with *homophily* and *preferential attachment*. Success at learning these characteristics is tested for eight state-of-the-art temporal graph learning models, using a range of empirical and synthetic test datasets—in total, over 6,500 models were trained in our experiments. Our results, summarized in Table 1, illustrate both strengths and some striking limitations of popular state-of-the-art models, and, at the same time, provide insights for the

---

\*Equal contribution. Author order among the co-first authors may be adjusted for individual use.

	CAWN	DyG-Former	DyRep	Graph-Mixer	JODIE	TCL	TGAT	TGN
Temporal Granularity	~	~	✓	✓	✓	~	~	✓
Direction	~	~	~	~	~	~	~	~
Density	✗	✗	✗	✗	✗	✗	✗	✗
Persistence	✓	✓	✗	~	✗	~	✓	✗
Periodicity	✗	✗	✗	✓	~	✓	~	~
Recency	✗	✗	✗	✗	✗	✗	✗	✗
Homophily	~	~	✓	~	✗	~	~	✗
Preferential Attachment	✓	✓	✓	✓	✓	✓	✓	✓

Table 1: **Summary of our experiments.** We test whether eight state-of-the-art temporal graph learning models (columns) learn important characteristics of temporal graphs (rows). A ✓ indicates success, ✗ failure, and ~ limited ability to learn a characteristic. Overall, we find consistent limitations in these models, such as their inability to distinguish directions of edges or lack of emphasis on recently active edges when predicting future links. At the same time, we find that models consistently learn preferential attachment to popular nodes in link formation and identify differences in their capacity to learn other characteristics.

practical application of graph learning models. We believe that our work can increase understanding and inspire more interpretability-focused evaluations of temporal graph learning models.

## 2 Background

Before describing our experiments, we briefly introduce key concepts of our work and summarize related research.

### 2.1 Preliminaries

**Temporal Graphs.** In literature, temporal graphs are typically modeled either as continuous-time or discrete-time graphs [12, 29].

In the continuous-time setting, the temporal graph can be considered as a stream of edges with fine-grained timestamps. A graph  $\mathcal{G}$  can be modeled as a tuple  $\mathcal{G} = (\mathcal{V}, \mathcal{E})$ , where  $\mathcal{V} = \{1, \dots, N\}$  denotes the set of all nodes,  $\mathcal{E} = \{(u_i, v_i, t_i)_{i \in \{1, 2, \dots\}}\}$  the set of edge events,  $u_i, v_i \in \mathcal{V}$  the source and destination nodes respectively, and  $t_i$ , with  $t_i \leq t_{i+1} \forall i$ , the timestamp of an edge event.

For the discrete-time setting, a temporal graph is instead considered as a series of static graph snapshots with a single timestep representing a longer time period. A graph  $\mathcal{G}$  is typically modeled as a sequence of graph snapshots  $\mathcal{G} = (\mathcal{G}_t)_{t \in \{1, 2, \dots, T\}}$ , where each snapshot corresponds to a tuple  $\mathcal{G}_t = (\mathcal{V}_t, \mathcal{E}_t)$  with  $\mathcal{V}_t$  denoting the nodes,  $\mathcal{E}_t$  the edges at time  $t$ , and  $T$  the total number of snapshots.

Datasets can be transformed between the two graph settings, although transformation from continuous to discrete-time typically causes some information loss when binning highly granular timestamps to discrete timesteps [12]. For the scope of this work, we focus on models designed for continuous-time dynamic graphs, as these are now more commonly used within the research community. However, we will often consider datasets with discretized timesteps due to our specific experimental designs. Within the scope of this work, unless otherwise specified, we generally ignore the use of edge and node features to simplify notation.

**Representation Learning for Temporal Link Prediction.** Most state-of-the-art graph learning models for dynamic graphs are based on different kinds of neural networks, from recurrent neural networks [14], to graph neural networks [20] and graph transformers [28]. During training, continuous-time models receive the sequence of edges  $\mathcal{E}$  up to a time  $t$  as input and learn a time-aware representation  $z_v^t \in \mathbb{R}^D$  for each node  $v \in \mathcal{V}$ . For dynamic link prediction, the input edges are directly used as positive examples, and optimized such that the existence of an edge  $(u, v)$  at test time  $t' \geq t$  can be predicted from the corresponding pair of representations  $z_u^t, z_v^t$ . There is some technical complexity in this optimization, as most models also require negative, i.e., non-existent edges, in training. Using all negative edges is typically infeasible since the size of the training data grows quadratically with the number of nodes. Further, empirical social networks are typically very sparse, such that models would be prone to predicting all edges as negative. Instead,

a set of negative training edges needs to be sampled [26]. This is further complicated in the temporal context by also needing to consider issues such as the timestamps of negative samples, whether or not to specifically sample edges which have been present previously and whether to include nodes which will only become active at a future timestamp. Similar issues also carry over to the model evaluation, where negative samples are incorporated in any test set. In the literature, it is often the case that, for each positive edge, a negative edge at the same timestamp is sampled, but there are more complex strategies such as explicitly sampling from previously positive edges [28].

### 2.2 Related Work

**Dynamic Graph Learning Benchmarks.** While popular general graph learning benchmarks, such as *Open Graph Benchmark* [9], also include link prediction tasks with time-based splits, benchmarks specifically targeting temporal graphs have emerged in recent years. Most notably, *Temporal Graph Benchmark (TGB)* [11] and *BenchTemp* [10] evaluate temporal graph learning models on node, link and graph classification tasks, showing that although strong results can be achieved on most datasets, there is no single solution across distinct datasets. *TGB* was later extended to heterogeneous and knowledge graphs by Gastinger et al. [6]. Yi et al. [27] identified limitations of temporal graph learning models in capturing sequential patterns in data, and established a benchmark focused on such data, while Gravina and Bacciu [7] built separate benchmarks for spatio-temporal, discrete-time and continuous-time graph datasets. The distinction between discrete and continuous-time models is bridged by Huang et al. [12], who present a unified framework and find that, despite some information loss, discrete-time models yield competitive results compared to continuous-time models, while being orders of magnitude faster at inference.

**Limitations of Temporal Link Prediction Models.** Several works have identified limitations in link prediction evaluation and the predictive capabilities of temporal graph learning models. Poursafaei et al. [18] found that strong performances in dynamic link prediction is often explained by task simplicity, as evidenced by their *EdgeBank* baseline. *EdgeBank* predicts a positive edge at test time if and only if it was observed in training, yielding similar accuracy to state-of-the-art methods on several datasets. Thus, *EdgeBank* was also included in benchmarks such as *TGB* [11] and *BenchTemp* [10]. Lampert, Blöcker, and Scholtes [15] further demonstrated that batch-based evaluation protocols can skew reported performance. Rahman, Modell, and Coon [19] revealed limitations of temporal graph learning models in learning temporal patterns, as perturbations such as repeating positive edges with slightly altered timestamps or shuffling timestamps among training edges often have minimal impact on performance. Cornell et al. [5] showed that simple heuristics favoring links to popular or recently active nodes can outperform state-of-the-art models on several datasets from *TGB* and *BenchTemp*. Further, they identified flaws in evaluation practices: commonly used rank-based metrics computed on sampled edge sets can yield results inconsistent with rankings on the full edge sets. In a broader context, Bechler-Speicher et al. [2] warned that poor benchmarking could lead to graph learning as a field losing relevance.

## 3 Experimental Framework

In Section 4, for each studied characteristic we systematically introduce the approach behind our evaluation, and follow it immediately with the findings. Within this section, we discuss experimental decisions that impact multiple characteristic experiments. Further, we provide the code used for our experiments on <https://github.com/dess-mannheim/tgl>.

**Datasets.** In our experiments, we selected datasets specific to each characteristic, using both empirical and synthetic data. As empirical datasets, we chose the *Bitcoin-Alpha* [13], *Enron* [21], *UCI* [17] and *Wikipedia* [14] datasets, due to both their popularity in related work and computationally reasonable size in light of the extensiveness of our experiments. For these datasets, we follow Huang et al. [12] for discretizing the timestamps, going from UNIX timestamps to monthly, weekly or hourly granularity. The impact of this discretization is explored as the first characteristic under temporal granularity in our experiments (see Section 4.1). More details on the datasets are provided in Appendix A.1. For the temporal granularity, direction and density characteristics, the empirical datasets were split into training, validation, and test data based on these discretized timesteps, with the first 70% of times being used as training data, and the remaining 30% evenly split into validation and test data. For the other characteristics, we designed synthetic graphs with direct correspondence to the studied characteristic and present these in the relevant results section.

**Models and Training Setup.** In our framework, we consider DyGFormer [28], GraphMixer [3], DyRep [22], JODIE [14], TGN [20], TCL [23], TGAT [25] and CAWN [24], using the implementations from DyGLib [28]. As hyperparameters, we used fixed values which gave effective performance on the empirical datasets. The values are set out in Appendix A.2, together with details of limited hyperparameter tuning in Appendix C. Unless noted otherwise, models were trained with accuracy on validation data used as early stopping criterion. Where validation data was not logically related to the training data, the training loss was used instead. We trained models ten times on each dataset, using different training seeds, or five times for each of five generation seeds for synthetic datasets. When not using the benchmark evaluation, testing is based on predictions for all possible edges at test time.

	Bitcoin-Alpha			Enron			UCI			Wikipedia		
	Cont.	Disc.	Flat	Cont.	Disc.	Flat	Cont.	Disc.	Flat	Cont.	Disc.	Flat
<b>CAWN</b>	0.780	0.984	0.728	0.959	0.941	0.518	0.968	0.953	0.684	0.989	0.983	0.571
<b>DyGFormer</b>	0.862	0.989	0.724	0.952	0.939	0.751	0.964	0.960	0.532	0.988	0.980	0.495
<b>DyRep</b>	0.893	0.905	0.941	0.891	0.732	0.576	0.925	0.889	0.834	0.965	0.943	0.829
<b>GraphMixer</b>	0.997	0.993	0.439	0.951	0.871	0.451	0.983	0.917	0.477	0.975	0.945	0.435
<b>JODIE</b>	0.999	0.999	0.961	0.936	0.860	0.701	0.958	0.946	0.845	0.969	0.955	0.829
<b>TCL</b>	0.880	0.991	0.668	0.842	0.870	0.580	0.956	0.949	0.624	0.971	0.952	0.549
<b>TGAT</b>	0.838	1.000	0.582	0.756	0.875	0.496	0.869	0.926	0.463	0.968	0.960	0.506
<b>TGN</b>	0.995	0.999	0.955	0.908	0.889	0.598	0.982	0.948	0.794	0.985	0.971	0.848

Table 2: **Temporal Granularity: impact of granularity of timestamps on performance.** We show average ROC-AUC of graph learning models on benchmark test sets for varying time granularities. *Cont.* indicates models were trained on the original data with UNIX timestamps, *Disc.* indicates data with discretized timestamps, and *Flat* denotes training data where all timestamps were set to 1. We observe that models generally improve their performance when more granular timestamps are given (✓). However, *CAWN*, *DyGFormer*, *TCL* and *TGAT* do not seem to benefit from using continuous over discretized timestamps (∼).

## 4 Results

In the following, we provide in-depth descriptions of our experiments for each characteristic, along with the corresponding findings. For each model, we give an assessment of whether they learn a characteristic (✓), learn it to a limited degree (∼), or do not learn it (✗). Results are also summarized in Table 1.

### 4.1 General Graph Features

We begin by presenting our experiments regarding *temporal granularity*, *direction*, and *density*.

#### 4.1.1 Temporal Granularity

The timestamps of edges in continuous-time datasets are typically highly granular, often down to the minute or even the second. This granularity is also typically assumed for link prediction at inference time, suggesting that predictions for very exact points in time can be made. To challenge this assumption, we investigate the effects of both using more discrete timesteps and essentially removing temporal information altogether.

**Approach.** For the three empirical datasets, we consider the following variants on which models are trained and tested:

1. *Continuous*: the original datasets with UNIX timestamps.
2. *Discrete*: the discrete-time variants of the datasets, following Huang et al. [12].
3. *Flattened*: variants with the timestamps of all training edges set to 1, validation edges to 2, and test edges to 3.

Training and evaluation is done using training and test splits based on the discrete version, such that no edge moves between groups. This avoids single timesteps being separated into different splits.

**Findings.** Table 2 shows the results across models and datasets for varying granularity. Flattening timestamps consistently harms performance to a severe degree. This is a strong indicator that temporal information relevant for the link prediction is present and that the models use this information to produce improved predictions. However, not all models appear to benefit from highly granular timestamps. Specifically, *TGAT* tends to perform best with discrete timesteps, while *CAWN*, *DyGFormer* and *TCL* appear to only be weakly impacted, or even perform best with discrete timesteps on Bitcoin-Alpha. Thus, we conclude that these models learn temporal granularity to a limited degree (∼). Conversely, *GraphMixer* and *DyRep* appear to deteriorate the most in performance when timestamps are discretized, and we conclude that these, along with the remaining models, learn temporal granularity (✓).

#### 4.1.2 Direction

In many empirical networks, edge direction is important: such as when encoding a signal sent from a source to a destination node. In graph learning models, direction is typically implied by node order, though directionality is not always explicitly assumed. Consequently, during inference, predicted edge probabilities are not necessarily symmetric with respect to node order.

## What Do Temporal Graph Learning Models Learn?

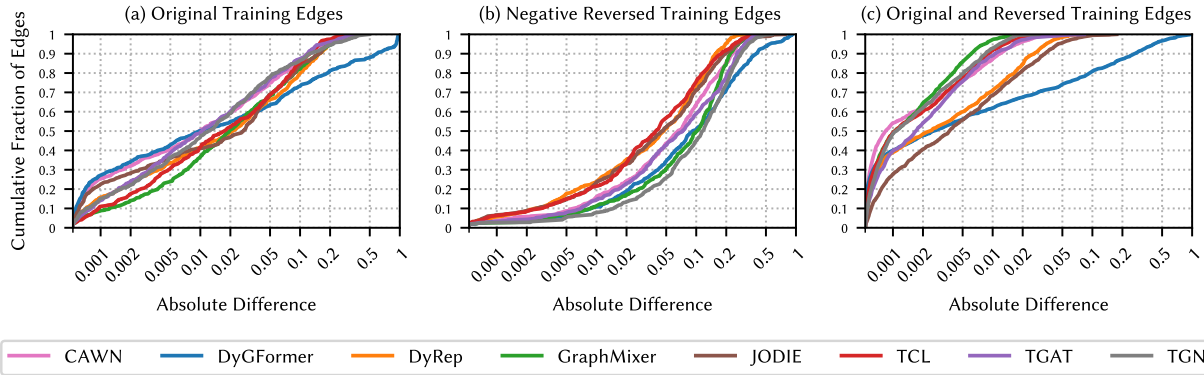


Figure 1: **Direction:** ability of graph learning models to distinguish edge directions. For each positive edge  $(u, v)$  in the UCI test data, we take the probability predicted by the graph learning models and compute the absolute difference to the predicted probability for the non-existing reverse edge  $(v, u)$ . Panel (a) depicts the cumulative distribution of the distance values when training with the original training edges, panel (b) shows these values when reverse edges of positive edges are provided as negative training samples, and panel (c) shows these values when, within training, both positive and negative edges are provided in both directions. We observe in (a) that, for most models, for roughly 50% of all edges the probability of edges being predicted is nearly symmetric with a difference smaller than 0.02. When reverse edges are explicitly provided as negatives, these edge differences, however, increase, with the share of edges with difference smaller than 0.02 reducing to roughly 30%. Conversely, training bidirectional edges increases symmetry in predictions, with 90% of all edges having a difference less than 0.01 for many models, and only *DyGFormer* yielding high differences. Overall, this indicates limited ability of models to learn direction ( $\sim$ ).

**Approach.** To identify whether temporal graph learning models indeed learn the direction of edges, we train them on the discretized empirical datasets under the following different training settings:

1. *Original:* we use the original training edges  $(u, v, t)$ ,
2. *Directed:* for each positive training edge  $(u, v, t)$ , we add the reverse edge  $(v, u, t)$  as *negative* edge to the training data,
3. *Undirected:* we make both positive and negative edges bidirectional by adding their reverse edges to the training data.

Through this, we aim to explore the degree to which predictions of positive edges  $(u, v, t)$  and their negative reverse edges  $(v, u, t)$  differ. If models learn directionality, this difference should be noticeable in the original setting, or at least if their reverse edges are explicitly negative. Conversely, explicitly learning both directions should impact the probability scores of reversed edges as well, ideally nullifying this difference. In all cases, we aimed to maintain (roughly) a 1:1 ratio of positive edges to randomly sampled negative edges, excluding the negative reverse edges in the *directed* setting. Evaluation was done on the regular discretized test data: see Appendix A.3 for more details.

**Findings.** We depict results for UCI in Figure 1—these are largely consistent with results on other datasets (cf. Apdx. B). For the original training data with implied directionality, we observe that most models assign highly similar probabilities to true edges  $(u, v, t)$  and the negative reverse edge  $(v, u, t)$  at testing time. For roughly half of the edges, the probability scores differ by less than 0.02, and, except for *DyGFormer*, it is only for less than 20% of the positive edges that these differences are bigger than 0.1. When providing explicitly directed edges during training, differences in probability scores between reverse edges generally tend to increase to a moderate but noticeable degree. Conversely, when always including both directions of an edge in the training data, we obtain nearly symmetric predictions across all positive edges. The only exception is *DyGFormer*, which still yields differences bigger than 0.1 in the probability scores. Overall, we conclude that models have no intrinsic notion of edge direction, but explicitly providing edge directions in training can steer outcomes to more or less symmetric prediction outcomes ( $\sim$ ).

### 4.1.3 Density

Link prediction benchmarks typically evaluate the performance of graph learning models on only a small subset of all possible links—this is also done because a full evaluation would be extremely expensive computationally. However, as

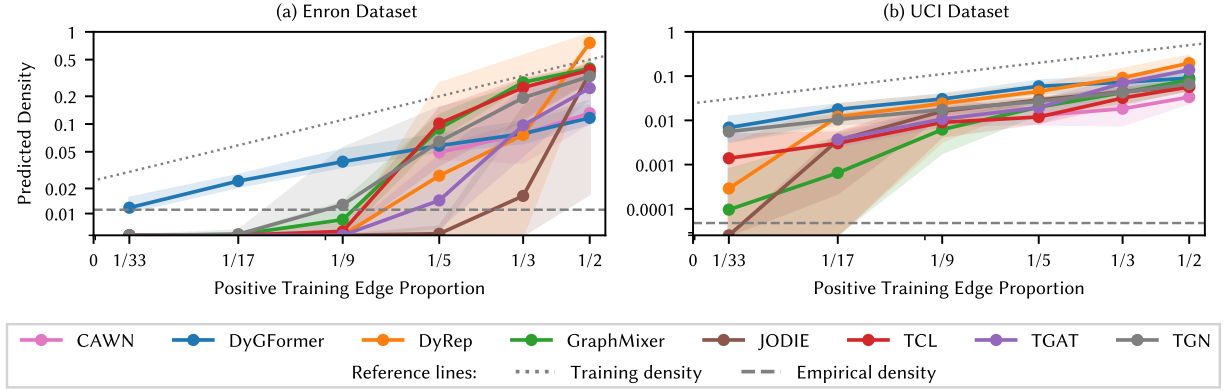


Figure 2: **Density:** *ability of models to replicate true density of networks.* We trained on the same set of positive training edges, but varied the negative sampling ratio. We depict the density resulting from predicting on all potential edges. Predicted density is generally much lower than the density seen during training. True density also appears hard to approximate, as models seem prone to predicting no edges when seeing larger numbers of negative edges. Thus, models do not appear to learn density (X).

a result it remains unclear whether models can grasp the density of a network, which is one of the most fundamental graph characteristics.

**Approach.** To evaluate whether graph learning models learn the density of a graph, we train the models on the discretized empirical datasets and vary the number of negative training edges during training, starting from a 1:1 ratio of training to test edges, and doubling the negative edges successively—for CAWN, this was limited to a maximum of 1:4, since more training data would exceed 80GB VRAM. Intuitively, a model should either naturally mimic the true density, or the predicted density should be proportional to the ratio of positive to negative training edges, which is the only explicit signal for density during training.

**Findings.** In Figure 2, we observe that the predicted density is generally much lower than the training ratio of positive to negative edges across all models. On the one hand, this indicates that models tend to learn that the training ratio of positive to negative edges does not represent the true link structure of a network. However, for commonly used training ratios of positive to negative edges, the true density of a network is overestimated by several orders of magnitude. Even when decreasing the ratio of positive nodes, it seems very hard to approximate the true density. Predicted density does not decrease proportional to an increasing number of negative training samples, and eventually models appear prone to simply predicting all edges as negative. Further, even if by chance a sweet spot is found, such as for *DyGFormer* at a 1:32 ratio on Enron, finding this sweet spot comes at a very high computational cost—this example takes 16 times the original training data, and this does not include the cost induced by the search.

Overall, this indicates that the models under study do not learn density (X). This finding bears some implications for practical application settings. In the context of recommenders, the given overestimation may be less of a problem, since rankings of edges are used rather than binary predictions. However, in settings where accurate prediction of future interactions is crucial, recalibration of the output probability scores may be needed.

## 4.2 Temporal Patterns

Next, we evaluate the ability of temporal graph learning models to learn *persistence*, *periodicity*, and *recency*.

### 4.2.1 Persistence

Persistent link patterns often occur in empirical data, and, intuitively, these should be trivial to learn. Thus, we investigate whether temporal graph learning models can reproduce such patterns, considering the extreme case of fully constant graphs.

**Approach.** We create fully persistent graphs by sampling a single snapshot from an empirical dataset and replacing all other timesteps with it. All nodes that are not present at the sampled snapshot are excluded from the network, and during training, negative samples are redrawn at every timestep. For evaluation, we compare between aggregate predicted probabilities of edges that exist in the snapshot and all other edges that could exist between the given nodes.

## What Do Temporal Graph Learning Models Learn?

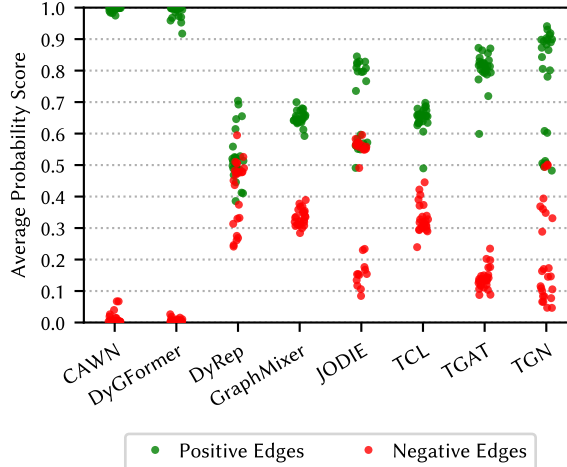


Figure 3: **Persistence:** *ability of models to learn persistent graphs.* We trained the graph learning models on fixed snapshots from the UCI dataset, which were repeated throughout training, and depict average probability scores resulting from each model when predicting positive and negative edges of these snapshots. Only *CAWN*, *DyGFormer* and *TGAT* appear to reproduce fixed graphs with reasonable confidence (✓).

**Findings.** In Figure 3, we present aggregated confidence scores of positive and negative edges on the UCI dataset, which are generally in line with the other datasets and the corresponding accuracy scores in Appendix B. Overall, there are stark differences in the capability of the models to learn persistence. On the positive side, *CAWN* and *DyGFormer* appear to perfectly learn the constant graph, while *TGAT* also distinguishes edges between timesteps with high confidence (✓). Similarly, *GraphMixer* and *TCL* also appear to discriminate edge groups in their aggregated probabilities, but do not show the same high level of confidence that could be expected for this task (∼). Conversely, *DyRep* appears to struggle identifying persistent edges, and both *JODIE* and *TGN* misclassify a lot of edges despite the trivial datasets (✗).

### 4.2.2 Periodicity

Going beyond completely constant networks, we now move to networks with repeating patterns. Temporal graph learning models should, intuitively, also be able to identify periodic patterns, i.e., networks which repeat their edges every  $k$  timesteps.

**Approach.** We create graphs with period length  $k \in \{2, 5\}$  from empirical networks by sampling an initial timestep at which the current and subsequent  $k - 1$  snapshots are taken. We then replace the original  $T$  timesteps by repeating this sequence of  $k$  snapshots  $\lceil T/k \rceil$  times. From this, for  $k = 2$ , each pair of continuously repeated snapshots yields four groups of edges: (i) edges which appear at both timesteps, (ii) edges which only appear at odd timesteps, (iii) edges which only appear at even timesteps, and (iv) edges which never appear. In our evaluation, we distinguish predictions for these groups of edges, and consider predictions at odd and even timesteps. For  $k = 5$ , the analysis is similar, see Appendix B.

**Findings.** Results for periodicity in terms of confidence scores on the UCI dataset are depicted in Figure 4. These are largely in line with the results for other datasets, period lengths, and the corresponding accuracy scores in Appendix B. We observe some differences compared to our experiments on persistence. Most notably, *CAWN* and *DyGFormer* do not appear to distinguish between odd and even timesteps, and simply give high confidence to every edge that occurs at all (✗). This behavior is very similar to how the *EdgeBank* baseline [18] would perform. Similarly, *DyRep* does not appear to distinguish between odd and even timesteps (✗). By contrast, *GraphMixer* and *TGAT* appear to distinguish odd and even timesteps very well (✓). Finally, *JODIE*, *TGAT* and *TCL* appear to consistently separate edges from different timesteps, but tend to be too confident in predictions on edges from the wrong timestep (∼).

### 4.2.3 Recency

For all deep learning models, it is often anticipated that models are more influenced by the latest data in training. This is even more of a consideration when the data itself contains a temporal element, as with dynamic graphs. Recent work has also shown that heuristics which emphasize predicting edges on more recently active nodes can perform very

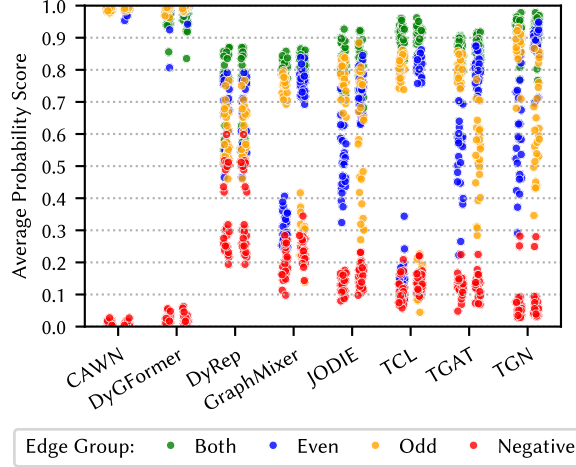


Figure 4: **Periodicity:** *ability of models to learn periodically repeated edges.* We selected pairs of consecutive snapshots from the UCI dataset, and tested whether the temporal graph learning models could reproduce a consistent pattern of two oscillating snapshots. We depict average predicted probabilities when testing at odd (left) and even (right) timesteps, colors correspond to predictions on edges present at odd, even, both, or neither timestep. Only *GraphMixer* and *TCL* appear to properly reproduce the training pattern (✓).

strongly on graph datasets [5]. Thus, we look to evaluate the extent to which model predictions are biased toward more recently seen data.

**Approach.** To evaluate a model’s ability to learn *recency*, we create datasets of 10 timesteps with disjoint sets of edges, and evaluate whether more recently seen edges have a higher probability score than earlier edges. These datasets are related to three empirical datasets by taking the number of edges at a representative timestep and sampling the same number of edges uniformly at random from all potential edges. This is done for each timestep successively, without replacement. In negative sampling, we exclusively sample edges which are not positive at any timestep. For both positive and negative edges, only one direction of each edge is considered for sampling. Thus, edge probabilities cannot be biased by some positive edges also being chosen as negative examples at other timesteps. No validation data is used, as there is no explicit connection between different timesteps. Predictions are made at time  $t = 10$ .

**Findings.** In Figure 5, we observe that, across all models and datasets, average probability scores of seen edges do not appear to vary based on the time they were last observed. Instead, they stay largely constant, with the exception of *TGAT* which appears to have some bias toward earlier edges on the Wikipedia-based graphs. This indicates that, in general, models do not place any predictive weight into the recency of edges (✗). Since edges were sampled completely at random, there is no additional information for models based on which predictions could be made and models consequently display high uncertainty in their probability scores. Given that heuristics based on predicting edges to recently active nodes often perform on par with state-of-the-art models [5], we argue that this yields potential room for improvement of this state-of-the-art. Introducing parameters that control whether a model places more weight on recent observations could improve performance on many datasets.

### 4.3 Mechanisms in Edge Formation

Finally, we show results on *homophily* and *preferential attachment*.

#### 4.3.1 Homophily

Homophily refers to the phenomenon that ‘birds of a feather flock together’. Here attention is paid to whether edges are between individuals from the same or different groups. Models should be able to learn the homophily of a graph since they receive the group information and all edge data.

**Approach.** To examine whether the models learn homophily, we use homophilic and heterophilic *stochastic block models (SBMs)* [8] with 1000 nodes, split into two groups of 500. For homophilic SBMs, we set the likelihood of inter-group links to  $p = 0.001$  and intra-group links to  $p = 0.005$ : reversed for heterophilic SBMs. Based on these parameters, we created dynamic networks of  $T = 100$  timesteps by resampling edges  $T$  times. Intuitively, if a model

## What Do Temporal Graph Learning Models Learn?

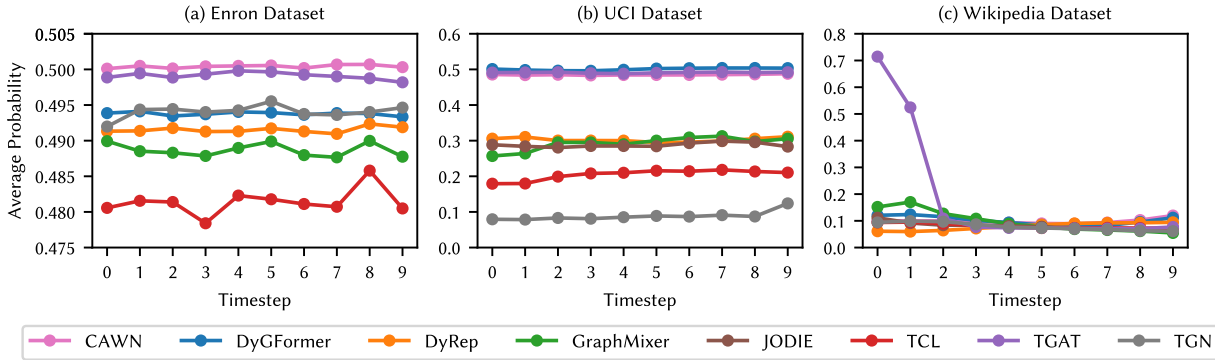


Figure 5: **Recency:** *impact of time that an edge was last seen on its probability score at test time.* For 10 timesteps, we sampled a random set of positive edges. These edge sets are disjoint over all timesteps, and reflect the density at representative timesteps in the original corresponding dataset. We show average predicted probability scores at timestep  $t = 10$  for all positive edges seen during training, separated by the timestep in which they were seen. Overall, we observe that there is no consistent trend regarding whether more recently (or earlier) edges have higher probability scores ( $\times$ ). Instead, all edges appear to have very similar probability scores on average, with the exception of *TGAT* on the graphs relating to the Wikipedia dataset.

learns homophily, it should mimic the edge formation of the homophilic SBM by placing higher likelihood on predicting intra-group rather than inter-group edges, with intra-group links for both groups being equally likely—showing opposite behavior for heterophilic SBMs. We test this assumption by aggregating predicted probabilities of edges within and between groups. During training, the node groups are explicitly provided as one-hot-encoded node features.

**Findings.** Table 3 presents the average predicted edge probabilities as well as the share of edges predicted to be positive within all combinations of intra-group and inter-group links in both the homophilic and the heterophilic settings. We observe that except for *JODIE* and *TGN* ( $\times$ ), all models appear to properly distinguish inter-group and intra-group links, even if predicted edge probabilities are not perfectly proportional to the model probabilities. However, when considering actual predictions, it appears that these models have converged to either predicting all edges of a group as positive, or all edges as negative, which does not reflect the nature of the SBMs. This extreme disparity is also reflected in the rankings of the top  $k$  most likely edges (see Apdx. B, Table 8). The only exception is *DyRep*, which actually predicts existence of minority edges. Thus, we conclude that except for *DyRep* ( $\checkmark$ ), all models other than *JODIE* and *TGN* learn homophily to a limited degree ( $\sim$ ).

Table 3: **Homophily:** *ability of models to reproduce homophily in edge formation.* We train graph learning models on stochastic block models with two groups (0 and 1) considering both homophilic and heterophilic graphs, with intra-group being five times more likely than inter-group links and vice versa. We depict the average confidence scores of all edges per group combination, and the share of all of edges per group which were predicted to exist. Except for *JODIE* and *TGN* ( $\times$ ), models generally distinguish intra-group and inter-group links ( $\sim$ ). However, only *DyRep* does not converge to fully binary deterministic predictions ( $\checkmark$ ).

Group	Homophilic SBM						Heterophilic SBM					
	Avg. Edge Probability			Fraction of Predicted Edges			Avg. Edge Probability			Fraction of Predicted Edges		
	0-0	0-1	1-1	0-0	0-1	1-1	0-0	0-1	1-1	0-0	0-1	1-1
<b>CAWN</b>	0.62	0.41	0.63	1.00	0.00	1.00	0.24	0.77	0.26	0.00	1.00	0.00
<b>DyGF.</b>	0.62	0.41	0.62	1.00	0.00	1.00	0.24	0.76	0.26	0.00	1.00	0.00
<b>DyRep</b>	0.61	0.33	0.55	0.74	0.35	0.62	0.41	0.67	0.24	0.10	0.86	0.09
<b>Mixer</b>	0.61	0.42	0.62	1.00	0.04	1.00	0.24	0.77	0.24	0.00	1.00	0.00
<b>JODIE</b>	0.81	0.17	0.40	0.91	0.00	0.40	0.71	0.73	0.02	0.91	0.88	0.00
<b>TCL</b>	0.62	0.40	0.62	1.00	0.00	1.00	0.24	0.77	0.26	0.00	1.00	0.00
<b>TGAT</b>	0.62	0.40	0.63	1.00	0.00	1.00	0.24	0.77	0.27	0.00	1.00	0.04
<b>TGN</b>	0.30	0.21	0.17	0.33	0.16	0.14	0.70	0.15	0.43	0.88	0.14	0.46

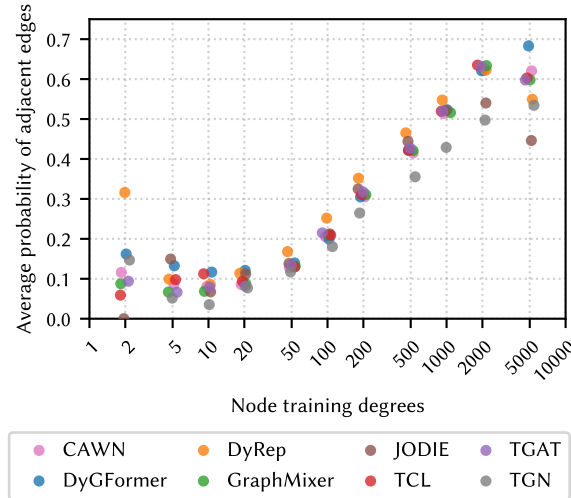


Figure 6: **Preferential Attachment:** *ability of models to reproduce preferential attachment in edge formation.* We trained all models on dynamic preferential attachment graphs over 100 timesteps. From the training graphs, we place the nodes into bins based on their logarithmic degree, and compute the average probability of all unseen edges adjacent to these nodes. The x-axis denotes the lower bound of the corresponding bins. We observe that for all models, average probabilities continuously increase with exponential increase of node degree. Thus, all models learn preferential attachment (✓).

### 4.3.2 Preferential Attachment

Preferential attachment refers to the phenomenon that high-degree nodes are more likely to receive new links. Given its commonality in empirical networks, it is of interest whether graph learning models learn this characteristic as well.

**Approach.** We create graphs based on the Barabási-Albert (BA) model [1] with 1000 nodes and 2000 edges at each timestep, for 100 training and 21 validation timesteps. The initial timestep is generated with the standard BA model to introduce variation in node degree. Subsequent timesteps add edges by sampling two nodes proportional to their number of previous edges—see Appendix A.4 for a formalization. Evaluation is done by examining the relationship between each node’s degree and the average probabilities predicted for its potential edges which were never positive in training. If preferential attachment is learned, then the edges connecting to nodes of high degree should receive higher average probabilities.

**Findings.** Results are presented in Figure 6. We observe that all models assign on average very low probabilities, around 0.1, to edges relating to low-degree nodes, and, with exponential increase of node degree, the average probability rises continuously up to 0.6-0.7. Most models have very similar average probabilities per bin, with only *TGN* tending to appear slightly lower than the rest. In addition, we see some slight outliers at the first and last bins, which could be attributed to the sparsity of these bins. Overall, the observed pattern is very reminiscent of the power-law degree distribution of the Barabasi-Albert model, and we conclude that all models indeed learn preferential attachment (✓). We replicate these results for a denser graph with 4000 edges per timestep in Appendix B.

## 5 Discussion and Conclusions

We close by summarizing our contributions, discussing limitations, and laying out potential avenues for future work.

**Contributions.** We propose a novel framework that assesses how well graph learning models capture intuitive characteristics of temporal networks. Based on this framework, we identify limitations of existing models: such as a limited distinction between the directions of edges, failure to detect periodic patterns, or a lack of emphasis on more recently observed graph dynamics. We do not argue that, in general, temporal graph learning models must capture all of these characteristics, as there may be application scenarios in which individual characteristics are not desirable or necessary. For instance, it may sometimes be counterproductive to place predictive emphasis on more recently seen edges. However, understanding a model’s predictive capabilities is crucial for selecting the right one in practice. In that sense, our work can be seen as both a benchmark for a more interpretability-driven evaluation of temporal

## What Do Temporal Graph Learning Models Learn?

graph learning models and, complementing existing performance-oriented benchmarks [6, 10, 11, 27], as an aid for researchers and practitioners when choosing a model for their task at hand.

**Limitations.** Overall, we conducted a very extensive set of experiments involving thousands of model runs across the eight graph characteristics that we evaluated. Given the extensive demands of these experiments, the number of datasets we used is naturally limited, and we do not argue that these datasets are representative.

Similarly, as a broad experimental study, theoretical analyses regarding the learning capabilities of models are out of scope for this work. However, our results could be used to draw some potential connections between the design and architecture of temporal graph models and their learning capabilities. For instance, a feature unique to *GraphMixer* is the fixed encoding scheme for the time span since the last edge signal, which is concatenated to link features in its link encoder. This encoding naturally captures periodic interactions, which was likely beneficial when learning periodicity. Similarly, this encoding may be beneficial when capturing temporal granularity. *CAWN* and *DyGFormer*, conversely, appear to weigh frequency of edges over temporal patterns in edge formation. While both apply time encoding conceptually similar to *GraphMixer*'s, they use learnable weights within it which may hinder optimal performance, and further, these temporal aspects may be overshadowed by *CAWN*'s walk correlation or *DyGFormer*'s neighbor co-occurrence encoding. These latter design choices might, by contrast, be beneficial for learning persistent patterns. These are, however, just a few among many architectural design choices of graph learning models which could explain the results for a small number of characteristics under study. Causal relationships could be explored in more principled manners in future work.

Further, for our experiments we focused on single isolated characteristics, even though real-world temporal graphs often exhibit multiple interacting characteristics. This design was, however, deliberate, as we aimed to minimize the likelihood of confounding effects. Combinations of characteristics may obfuscate what is really steering the predictions of graph learning models.

Finally, we relied on hyperparameter settings which proved effective on the empirical datasets used to probe density, direction, and temporal granularity. Especially when testing other graph characteristics, we cannot rule out that varying hyperparameters might influence results. However, additional ablation studies with varied hyperparameters in Appendix C showed no significant impact.

**Future Work.** Our work evaluates a broad range of graph characteristics, but the set is not conclusive. Future work could consider additional characteristics, or combinations. Similarly, our work does not include models for the discrete setting. Deploying such models in our framework would be a simple extension that could also uncover more general differences between these model classes.

Aside from additions to our framework, future work could pick up on the limitations we found in the ability of models to learn characteristics such as density, direction or recency, and focus on designing models which are able to learn these characteristics.

## Acknowledgements

This work is supported by the Deutsche Forschungsgemeinschaft (DFG, German Research Foundation) under Grant No. 453349072 and Grant No. 530081187. The authors acknowledge support by the state of Baden-Württemberg through bwHPC and DFG through grant INST 35/1597-1 FUGG.

## References

- [1] Albert-László Barabási and Réka Albert. “Emergence of Scaling in Random Networks”. In *Science* 286(5439), pp. 509–512, 1999.
- [2] Maya Bechler-Speicher, Ben Finkelshtein, Fabrizio Frasca, Luis Müller, Jan Tönshoff, Antoine Siraudin, Viktor Zaverkin, Michael M. Bronstein, Mathias Niepert, Bryan Perozzi, Mikhail Galkin, and Christopher Morris. “Position: Graph Learning Will Lose Relevance Due To Poor Benchmarks”. In *Proceedings of the 42nd International Conference on Machine Learning*, Proceedings of Machine Learning Research 267, pp. 81067–81089, Vancouver, Canada, 2025.
- [3] Weilin Cong, Si Zhang, Jian Kang, Baichuan Yuan, Hao Wu, Xin Zhou, Hanghang Tong, and Mehrdad Mahdavi. “Do We Really Need Complicated Model Architectures For Temporal Networks?” *International Conference on Learning Representations*, Kigali, Rwanda, 2023.
- [4] Filip Cornell, Oleg Smirnov, Gabriela Zarzar Gandler, and Lele Cao. “Are We Really Measuring Progress? Transferring Insights from Evaluating Recommender Systems to Temporal Link Prediction”. *Temporal Graph Learning Workshop @ KDD 2025*, Toronto, Canada, 2025.

- [5] Filip Cornell, Oleg Smirnov, Gabriela Zarzar Gandler, and Lele Cao. “On the Power of Heuristics in Temporal Graphs”. *I Can’t Believe It’s Not Better: Challenges in Applied Deep Learning, Workshop at the International Conference on Learning Representations*, Singapore, 2025.
- [6] Julia Gastinger, Shenyang Huang, Mikhail Galkin, Erfan Loghmani, Ali Parviz, Farimah Poursafaei, Jacob Danovitch, Emanuele Rossi, Ioannis Koutis, Heiner Stuckenschmidt, Reihaneh Rabbany, and Guillaume Rabusseau. “TGB 2.0: A Benchmark for Learning on Temporal Knowledge Graphs and Heterogeneous Graphs”. In *Advances in Neural Information Processing Systems 37*, pp. 140199–140229, Vancouver, Canada, 2024.
- [7] Alessio Gravina and Davide Bacciu. “Deep Learning for Dynamic Graphs: Models and Benchmarks”. In *IEEE Transactions on Neural Networks and Learning Systems 35*(9), pp. 11788–11801, 2024.
- [8] Paul W. Holland, Kathryn Blackmond Laskey, and Samuel Leinhardt. “Stochastic Blockmodels: First Steps”. In *Social Networks 5*(2), pp. 109–137, 1983.
- [9] Weihua Hu, Matthias Fey, Marinka Zitnik, Yuxiao Dong, Hongyu Ren, Bowen Liu, Michele Catasta, and Jure Leskovec. “Open Graph Benchmark: Datasets for Machine Learning on Graphs”. In *Advances in Neural Information Processing Systems 33*, pp. 22118–22133, Virtual Event, 2020.
- [10] Qiang Huang, Xin Wang, Susie Xi Rao, Zhichao Han, Zitao Zhang, Yongjun He, Quanqing Xu, Yang Zhao, Zhigao Zheng, and Jiawei Jiang. “Benchtemp: A General Benchmark for Evaluating Temporal Graph Neural Networks”. In *2024 IEEE 40th International Conference on Data Engineering*, pp. 4044–4057, Utrecht, Netherlands, 2024.
- [11] Shenyang Huang, Farimah Poursafaei, Jacob Danovitch, Matthias Fey, Weihua Hu, Emanuele Rossi, Jure Leskovec, Michael Bronstein, Guillaume Rabusseau, and Reihaneh Rabbany. “Temporal Graph Benchmark for Machine Learning on Temporal Graphs”. In *Advances in Neural Information Processing Systems 36*, pp. 2056–2073, New Orleans, LA, United States, 2023.
- [12] Shenyang Huang, Farimah Poursafaei, Reihaneh Rabbany, Guillaume Rabusseau, and Emanuele Rossi. “UTG: Towards a Unified View of Snapshot and Event Based Models for Temporal Graphs”. In *Proceedings of the Third Learning on Graphs Conference 269*, art. 28, Phoenix, AZ, United States, 2025.
- [13] Srijan Kumar, Francesca Spezzano, V. S. Subrahmanian, and Christos Faloutsos. “Edge Weight Prediction in Weighted Signed Networks”. In *16th IEEE International Conference on Data Mining*, pp. 221–230, Barcelona, Spain, 2016.
- [14] Srijan Kumar, Xikun Zhang, and Jure Leskovec. “Predicting Dynamic Embedding Trajectory in Temporal Interaction Networks”. In *Proceedings of the 25th ACM SIGKDD International Conference on Knowledge Discovery & Data Mining*, pp. 1269–1278, Anchorage, Alaska, United States, 2019.
- [15] Moritz Lampert, Christopher Blöcker, and Ingo Scholtes. “From Link Prediction to Forecasting: Addressing Challenges in Batch-based Temporal Graph Learning”. In *Transactions on Machine Learning Research*, 2026.
- [16] Juanhui Li, Harry Shomer, Haitao Mao, Shenglai Zeng, Yao Ma, Neil Shah, Jiliang Tang, and Dawei Yin. “Evaluating Graph Neural Networks for Link Prediction: Current Pitfalls and New Benchmarking”. In *Advances in Neural Information Processing Systems 36*, pp. 3853–3866, New Orleans, LA, United States, 2023.
- [17] Pietro Panzarasa, Tore Opsahl, and Kathleen M. Carley. “Patterns and Dynamics of Users’ Behavior and Interaction: Network Analysis of an Online Community”. In *Journal of the American Society for Information Science and Technology 60*(5), pp. 911–932, 2009.
- [18] Farimah Poursafaei, Shenyang Huang, Kellin Pelrine, and Reihaneh Rabbany. “Towards Better Evaluation for Dynamic Link Prediction”. In *Advances in Neural Information Processing Systems 35*, pp. 32928–32941, New Orleans, LA, United States, 2022.
- [19] Aniq Ur Rahman, Alexander Modell, and Justin Coon. “Rethinking Evaluation for Temporal Link Prediction through Counterfactual Analysis”. *I Can’t Believe It’s Not Better: Challenges in Applied Deep Learning, Workshop at the International Conference on Learning Representations*, Singapore, 2025.
- [20] Emanuele Rossi, Ben Chamberlain, Fabrizio Frasca, Davide Eynard, Federico Monti, and Michael Bronstein. “Temporal Graph Networks for Deep Learning on Dynamic Graphs”. *Graph Representation Learning and Beyond (GRL+), Workshop at the International Conference on Learning Representations*, Virtual Event, 2020.
- [21] Jitesh Shetty and Jafar Adibi. *The Enron Email Dataset Database Schema and Brief Statistical Report*. Marina del Rey, CA, United States: Information Sciences Institute, University of Southern California, 2004.
- [22] Rakshit Trivedi, Mehrdad Farajtabar, Prasenjeet Biswal, and Hongyuan Zha. “DyRep: Learning Representations over Dynamic Graphs”. *International Conference on Learning Representations*, New Orleans, LA, United States, 2019.
- [23] Lu Wang, Xiaofu Chang, Shuang Li, Yunfei Chu, Hui Li, Wei Zhang, Xiaofeng He, Le Song, Jingren Zhou, and Hongxia Yang. “TCL: Transformer-based Dynamic Graph Modelling via Contrastive Learning”. [arXiv:2105.07944](https://arxiv.org/abs/2105.07944), 2021.
- [24] Yanbang Wang, Yen-Yu Chang, Yunyu Liu, Jure Leskovec, and Pan Li. “Inductive Representation Learning in Temporal Networks via Causal Anonymous Walks”. *International Conference on Learning Representations*, Virtual Event, 2021.
- [25] Da Xu, Chuanwei Ruan, Evren Korpeoglu, Sushant Kumar, and Kannan Achan. “Inductive Representation Learning on Temporal Graphs”. *International Conference on Learning Representations*, Virtual Event, 2020.
- [26] Yang Yang, Ryan N. Lichtenwalter, and Nitesh V. Chawla. “Evaluating Link Prediction Methods”. In *Knowledge and Information Systems 45*(3), pp. 751–782, 2015.
- [27] Lu Yi, Jie Peng, Yanping Zheng, Fengran Mo, Zhewei Wei, Yuhang Ye, Yue Zixuan, and Zengfeng Huang. “TGB-Seq Benchmark: Challenging Temporal GNNs with Complex Sequential Dynamics”. *International Conference on Learning Representations*, Singapore, 2025.

- [28] Le Yu, Leilei Sun, Bowen Du, and Weifeng Lv. “Towards Better Dynamic Graph Learning: New Architecture and Unified Library”. In *Advances in Neural Information Processing System* 36, pp. 67686–67700, Vancouver, Canada, 2024.
- [29] Yanping Zheng, Lu Yi, and Zhewei Wei. “A Survey of Dynamic Graph Neural Networks”. In *Frontiers of Computer Science* 19(6), art. 196323, 2025.

## A Additional Details on Experimental Setup

### A.1 Details of Empirical Datasets

In our experiments with empirical data, we consider the following datasets:

1. *Enron* [21] is a network modeling email communication within the Enron corporation between 2000 and 2002. Nodes correspond to individuals that worked at Enron, and an edge  $(u, v, t)$  indicates that an email was sent from individual  $u$  to individual  $v$  at time  $t$ .
2. *Bitcoin-Alpha* [13] is a whom-trust-whom network of bitcoin users that traded on the platform <http://www.btc-alpha.com>. An edge  $(u, v, t)$  indicates that user  $u$  assigned a rating to user  $v$  at time  $t$ . Each edge further contains the rating score which ranges from -10 to 10.
3. *UCI* [17] represents an online community of students at the University of California, Irvine. Within this community, students could search each other’s profiles and message each other. The network is then modeled based on messages sent in the period from April to October 2004. An edge  $(u, v, t)$  indicates that user  $u$  sent a message to user  $v$  at time  $t$ .
4. *Wikipedia* [14] is a heterogeneous network that models one month of edits on Wikipedia pages. An edge  $(u, v, t)$  indicates that editor  $u$  edited page  $v$  at time  $t$ .

Additional details regarding the number of nodes, edges, and discrete timesteps are provided in Table 4.

### A.2 Choice of Hyperparameters

- Learning rate: 1e-4
- Batch size: 200
- Loss: BCELoss
- Optimizer: Adam
- Dropout: 0.0
- Max epochs: 300 (100 for Preferential Attachment)
- Early stopping tolerance: 1e-6
- Early stopping patience: 20
- Time feature dimension: 100
- Number of neighbors: 20
- Time gap for neighbors: 2000
- Number of layers: *TGAT, TCL, GraphMixer& DyGFormer- 2, JODIE, TGN& DyRep- 1*
- Number of heads: *TGAT, TCL, DyGFormer, JODIE, TGN& DyRep- 2*
- Number of walk heads: *CAWN- 8*

Table 4: **Statistics of empirical datasets.** We distinguish between number of edges in the original continuous datasets, and edges in the discretized versions, where duplicate edges in individual timesteps were removed.

Dataset	Nodes	Continuous Edges	Discrete Edges	Unique Edges	Discrete Timesteps
Enron	184	125,235	10,472	3,125	45 (monthly)
Bitcoin-Alpha	3,783	24,185	24,185	24,185	63 (monthly)
UCI	1,899	59,835	26,628	20,296	29 (weekly)
Wikipedia	9,277	157,474	65,085	18,257	745 (hourly)

Table 5: Average ROC-AUC of graph learning models across datasets and training variants.

	Bitcoin-Alpha			Enron					UCI					Wikipedia		
	Cont.	Disc.	Flat	Cont.	Disc.	DF	Flat	FF	Cont.	Disc.	DF	Flat	FF	Cont.	Disc.	Flat
<b>CAWN</b>	0.780	0.984	0.728	0.959	0.941	0.903	0.518	0.630	0.968	0.953	0.971	0.684	0.671	0.989	0.983	0.571
<b>DyGF</b>	0.862	0.989	0.724	0.952	0.939	0.922	0.751	0.639	0.964	0.960	0.972	0.532	0.463	0.988	0.980	0.495
<b>DyRep</b>	0.893	0.905	0.941	0.891	0.732	0.830	0.576	0.810	0.925	0.889	0.935	0.834	0.916	0.965	0.943	0.829
<b>Mixer</b>	0.997	0.993	0.439	0.951	0.871	0.823	0.451	0.459	0.983	0.917	0.944	0.477	0.518	0.975	0.945	0.435
<b>JODIE</b>	0.999	0.999	0.961	0.936	0.860	0.911	0.701	0.853	0.958	0.946	0.964	0.845	0.941	0.969	0.955	0.829
<b>TCL</b>	0.880	0.991	0.668	0.842	0.870	0.832	0.580	0.554	0.956	0.949	0.969	0.624	0.677	0.971	0.952	0.549
<b>TGAT</b>	0.838	1.000	0.582	0.756	0.875	0.844	0.496	0.488	0.869	0.926	0.925	0.463	0.491	0.968	0.960	0.506
<b>TGN</b>	0.995	0.999	0.955	0.908	0.889	0.912	0.598	0.904	0.982	0.948	0.971	0.794	0.915	0.985	0.971	0.848

- Position feature dimension: *CAWN*- 172
- Walk length: *CAWN*- 2
- Number of depths: *TCL*- 21
- Number of tokens: *GraphMixer*- 20
- Channel embedding dimension: *DyGFormer*- 50
- Patch size: *DyGFormer*- 2
- Max input sequence length: *DyGFormer*- 64

For the datasets and models we used, Yu et al. [28] found recent sampling of neighbors to always be the most effective. There was more variation in the other parameters depending on the dataset and model combination. The values fixed here give very similar Average Precision scores when following the DyGLib evaluation procedure compared to the optimal dataset specific hyperparameters specified in the paper (see Table 6).

### A.3 Training and Evaluation for Direction

For the direction experiment, we make changes to the data used to train the models. For the undirected dataset variant, we ensure that all edges are included in both directions i.e. if  $(u, v, t)$  appears as positive or negative then so must  $(v, u, t)$ . For the directed dataset variant, we ensure that if an edge  $(u, v, t)$  appears as a positive but the reverse edge  $(v, u, t)$  does not, then the reverse edge is included as a negative edge. In the case that there are  $n$  positive edges, we would normally use  $n$  sampled negative edges. To ensure at least this number of sampled negative edges is still also used, the models are trained with  $2n$  negative edges for this variant, where up to  $n$  may be the reverses of positive edges.

The evaluation for the direction experiment considers pairs of edges  $(u, v, t)$  with their corresponding reverse edge  $(v, u, t)$ , where  $(u, v, t)$  should be positive at the next timestep after training and validation and  $(v, u, t)$  should be negative. If the model could predict perfectly, then the difference between the predictions should be large. But, if direction is not learned then the edges might receive similar predictions.

### A.4 Preferential Attachment Model

At  $t = 0$ , a BA model is used with  $m = 2$  with 1000 nodes. This produces a network with 2000 edges. As additional nodes are added, the probability that node  $i$  is selected  $p_i$  for a new node to connect to is  $p_i = \frac{k_i}{\sum_j k_j}$  where  $k_i$  is the degree of node  $i$  and the sum is over all existing nodes  $j$ .

For each later timestep, no additional nodes are added to the graph and 2000 edges are added by sampling two nodes for each. The probability that node  $i$  is selected at time  $t = T$ ,  $p_i^T$ , is defined as  $p_i^T = \frac{\sum_{t=0}^{T-1} k_i^t}{\sum_{t=0}^{T-1} \sum_j k_j^t}$  where  $k_i^t$  is the degree of node  $i$  at time  $t$ .

## B Additional Plots and Tables

In the following, we present and discuss additional results from our experiments regarding *direction*, *persistence*, *periodicity*, *homophily*, and *preferential attachment*.

**Direction.** Figures 7 and 8 show results for the Enron and Bitcoin-Alpha datasets. In general, results are in line with those observed on the UCI dataset, cf. Figure 1: for the original training edges, most edge probabilities are very

## What Do Temporal Graph Learning Models Learn?

	Bitcoin-Alpha			Enron			UCI			Wikipedia		
	Cont.	Disc.	Flat	Cont.	Disc.	Flat	Cont.	Disc.	Flat	Cont.	Disc.	Flat
<b>CAWN</b>	0.745	0.986	0.675	0.958	0.945	0.497	0.976	0.952	0.694	0.992	0.986	0.589
<b>DyGFormer</b>	0.862	0.990	0.759	0.951	0.946	0.753	0.974	0.959	0.576	0.991	0.983	0.531
<b>DyRep</b>	0.896	0.866	0.927	0.872	0.654	0.556	0.921	0.875	0.817	0.968	0.944	0.822
<b>GraphMixer</b>	0.997	0.994	0.597	0.946	0.860	0.507	0.986	0.918	0.545	0.979	0.950	0.494
<b>JODIE</b>	0.999	0.999	0.951	0.920	0.815	0.642	0.955	0.939	0.828	0.972	0.958	0.817
<b>TCL</b>	0.896	0.991	0.693	0.861	0.860	0.577	0.966	0.946	0.649	0.979	0.957	0.578
<b>TGAT</b>	0.810	1.000	0.657	0.770	0.860	0.524	0.888	0.929	0.550	0.972	0.963	0.506
<b>TGN</b>	0.995	0.999	0.954	0.894	0.888	0.551	0.984	0.944	0.820	0.987	0.974	0.845

Table 6: **Temporal Granularity:** *impact of granularity of timestamps on performance.* We show the mean average precision of temporal graph learning models on benchmark test sets for varying time granularity. These reflect the same patterns seen for ROC-AUC in Table 2, with performance on the continuous datasets comparable to the values found by Yu et al. [28].

Dataset variant	Model	Bitcoin-Alpha				Enron				UCI			
		Edges	Both directions	Reverse edges	Other	Edges	Both directions	Reverse edges	Other	Edges	Both directions	Reverse edges	Other
Original	CAWN	0.92	-	0.92	0.03	0.80	0.89	0.79	0.23	0.73	0.83	0.72	0.10
	DyGFormer	0.87	-	0.67	0.03	0.79	0.89	0.78	0.19	0.77	0.86	0.80	0.13
	DyRep	0.83	-	0.83	0.16	0.62	0.63	0.62	0.54	0.73	0.80	0.74	0.31
	GraphMixer	0.91	-	0.91	0.03	0.71	0.77	0.69	0.42	0.71	0.81	0.71	0.15
	JODIE	0.88	-	0.88	0.01	0.60	0.63	0.60	0.33	0.71	0.81	0.70	0.08
	TCL	0.93	-	0.93	0.03	0.68	0.74	0.67	0.40	0.70	0.81	0.70	0.12
	TGAT	0.94	-	0.93	0.02	0.56	0.63	0.55	0.34	0.82	0.86	0.81	0.21
	TGN	0.92	-	0.92	0.02	0.72	0.80	0.71	0.37	0.83	0.88	0.81	0.10
Undirected	CAWN	0.94	-	0.94	0.02	0.87	0.95	0.87	0.33	0.77	0.84	0.77	0.13
	DyGFormer	0.94	-	0.94	0.02	0.83	0.92	0.83	0.22	0.80	0.85	0.82	0.13
	DyRep	0.84	-	0.84	0.15	0.65	0.67	0.65	0.53	0.79	0.85	0.79	0.26
	GraphMixer	0.93	-	0.93	0.01	0.65	0.70	0.65	0.41	0.80	0.84	0.80	0.17
	JODIE	0.90	-	0.90	0.01	0.57	0.59	0.57	0.33	0.71	0.79	0.71	0.10
	TCL	0.94	-	0.94	0.02	0.57	0.61	0.57	0.37	0.77	0.85	0.77	0.13
	TGAT	0.93	-	0.93	0.02	0.58	0.64	0.58	0.34	0.79	0.83	0.79	0.20
	TGN	0.94	-	0.94	0.02	0.67	0.75	0.67	0.37	0.82	0.87	0.82	0.14
Directed	CAWN	-	-	-	-	0.56	0.66	0.52	0.15	0.50	0.60	0.50	0.09
	DyGFormer	0.70	-	0.61	0.08	0.64	0.71	0.59	0.15	0.62	0.70	0.63	0.13
	DyRep	0.47	-	0.45	0.13	0.34	0.34	0.34	0.34	0.53	0.59	0.53	0.19
	GraphMixer	0.68	-	0.61	0.03	0.50	0.54	0.48	0.30	0.52	0.59	0.50	0.12
	JODIE	0.66	-	0.58	0.01	0.36	0.37	0.36	0.24	0.52	0.59	0.50	0.05
	TCL	0.71	-	0.62	0.02	0.46	0.49	0.44	0.28	0.52	0.61	0.51	0.11
	TGAT	0.70	-	0.59	0.02	0.39	0.42	0.38	0.28	0.56	0.63	0.56	0.13
	TGN	0.68	-	0.52	0.02	0.49	0.54	0.46	0.25	0.64	0.68	0.60	0.07

Table 7: **Direction:** *ability of graph learning models to distinguish directions of edges.* The average probability given to each edge by group, for each model and dataset variant combination for the Enron, Bitcoin-Alpha and UCI datasets, with 1:1 negative edges in training. There are no edges in Bitcoin-Alpha which appear in both directions in the testing timestep. There is generally very little difference in the average probability given to true edges and their reverse edges which should not appear. However, edges which should appear in both directions generally receive a higher average probability than those which should appear in only a single direction.

symmetric, but there are also higher values, specifically for *DyGFormer*. In the *directed* setting, providing a negative reverse training edge for each positive training edge tends to increase differences between positive test edges and their negative reverse, while always providing both directions in the *undirected* setting generally yields much more symmetric predictions. Yet, on Enron, it appears that in the directed setting, these differences tend to decrease for *DyRep*, *JODIE*, and *TGAT*. This is, however, likely due to the overall higher ratio of negative to positive sample pushing many edge probabilities toward 0. As observed in our experiments on *density*, an increase in negative samples will generally decrease the probabilities of edges being predicted as positive. We can also see in Table 7 how predicted edge probabilities in the *directed* setting are generally lower.

Table 7 further illustrates additional limitations in the ability of models to learn direction of edges. Generally, it would be desirable if the non-appearing reverses of positive edges would differ more strongly in their predicted probabilities from the true positive edges. When comparing the average probability scores of reverse positive edges in the *original*

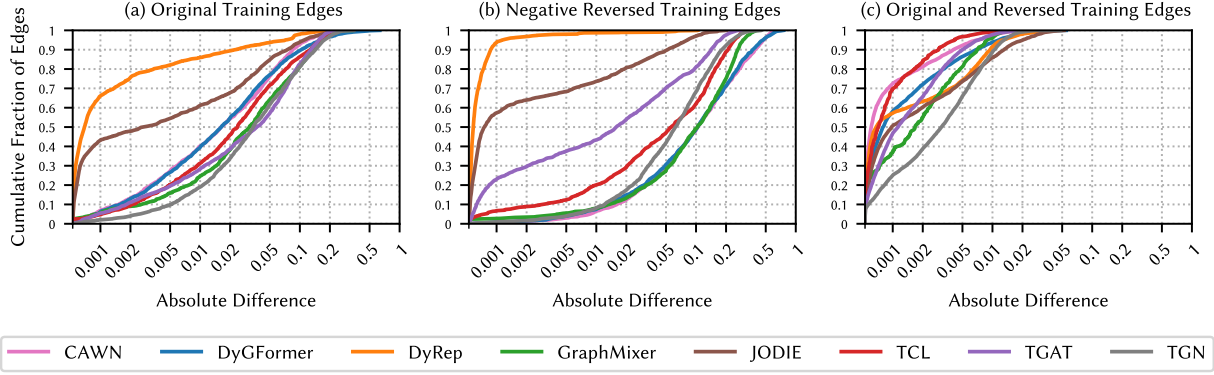


Figure 7: **Direction:** ability of graph learning models to distinguish edge directions. Additional results for the Enron dataset. *DyRep* and *JODIE* particularly struggle with distinguishing the two edge directions.

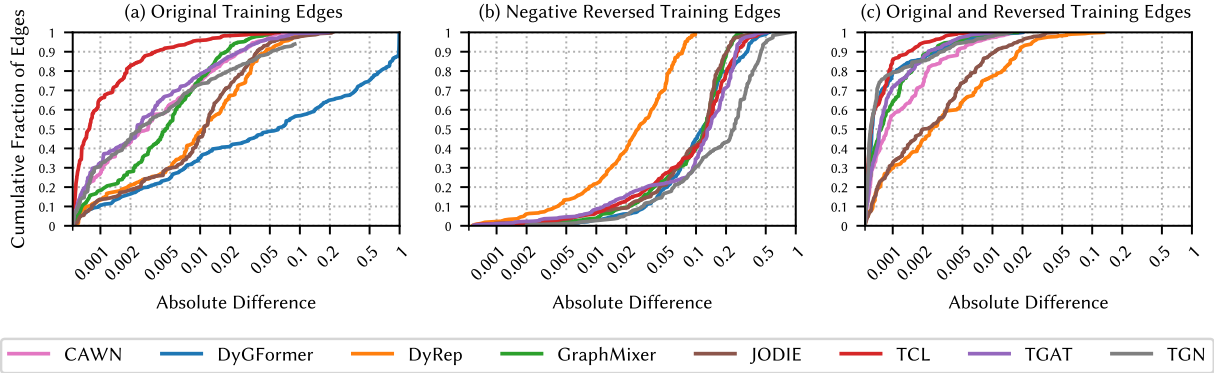


Figure 8: **Direction:** ability of graph learning models to distinguish edge directions. Additional results for the Bitcoin-Alpha dataset. Compared to the results on the UCI dataset in Figure 1, some models, apart from *DyGFormer*, are less able to distinguish edge pairs in the original dataset, but with improved results when reverse edges are explicitly provided as negatives. This might reflect the fact that this dataset never contains an edge in both directions at the same timestep.

setting, which are mostly between 0.7-0.8, we find a stark difference to those of all other negative edges which tend to vary between 0.1-0.2. Even more strikingly, for some models, the reverses of positive edges receive higher average probability scores than their true positive counterparts. While it is plausible that the probability of a signal between nodes which had a previous signal in either direction comes out higher than the probability of a signal between nodes which were never in contact, the reverse edge probabilities should still be more distinguishable from the true edges, and scores between 0.4-0.5 would appear to be more sensible estimations. Training in the *directed* setting appears to alleviate this to some degree specifically on Bitcoin-Alpha. For the other datasets, the averages appear less affected, however, this may also be due to many positive test edges having been observed in both directions during training, given the reciprocal nature of these communication networks, and the number of temporal links of these datasets in relation to the number of nodes.

**Persistence.** Figure 9 shows the cumulative fraction of positive and negative edges that are predicted for the Enron and Wikipedia datasets. These results are in line with the results on the data created from the UCI dataset, as reported in Figure 3 in the main text. Figure 10 shows the balanced accuracies across all datasets, which are surprisingly low considering the trivial nature of the given prediction task.

**Periodicity.** Figure 11 shows additional results with snapshots from the Enron and Wikipedia datasets. Results are mostly in line with those observed on the UCI dataset (see Figure 4). Yet, we see a few notable differences on Enron for *CAWN*, *DyGFormer*, and *JODIE*. First, *CAWN* and *DyGFormer* appear to distinguish different snapshots to some degree, which is not the case for the other datasets. A likely explanation is that these models base their predictions on the frequency of seen edges rather than temporal patterns. Enron has relatively few timesteps, especially compared to

## What Do Temporal Graph Learning Models Learn?

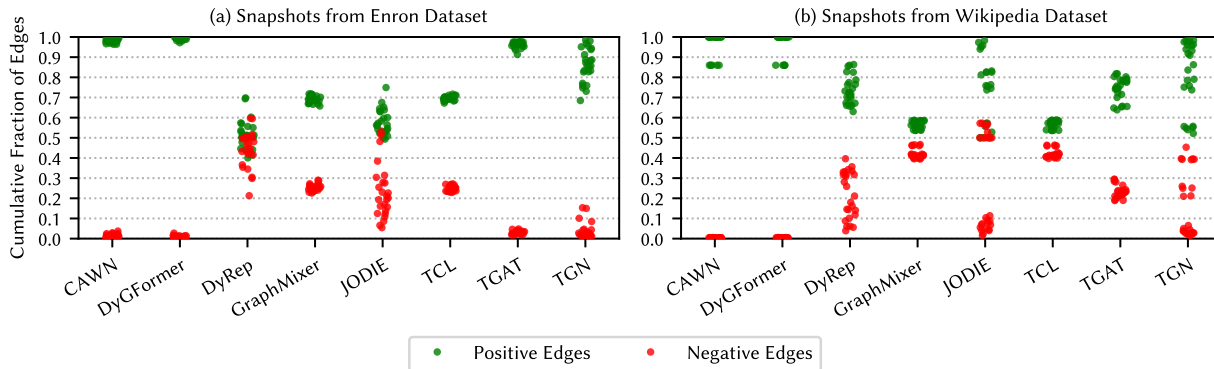


Figure 9: **Persistence:** *ability of models to learn persistent snapshots.* Additional results using snapshots from Enron and Wikipedia datasets. Only *DyGFormer* appears to consistently learn persistent networks, while *TGAT* appears to get the tendency right.

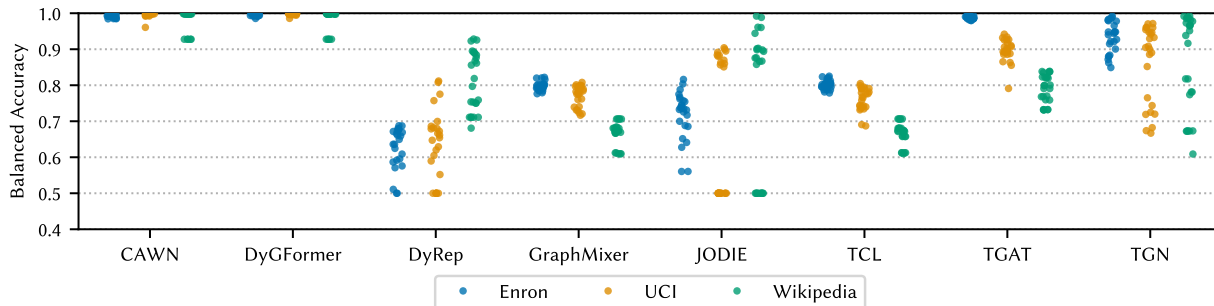


Figure 10: **Persistence:** *ability of models to learn persistent snapshots.* We show balanced accuracies of all models across all datasets and training seeds. Only *CAWN*, *DyGFormer* and *TGAT* appear to consistently learn persistent networks, other models struggle to varying degrees.

the 632 training snapshots for Wikipedia. Having seen those edges on a very frequent basis, these models converge to predicting all edges as similarly likely, invariant to the timestep. Thus, we conclude that these models do not learn periodicity (✗). *JODIE*, on the other hand, shows the opposite behavior, struggling on Enron where fewer snapshots are given, but picking up on the pattern the more it has been observed. Thus, we conclude that *JODIE* learns *periodicity* to a limited degree (∼).

These general trends are also consistent with the results for period length 5, as depicted in Figures 12 and 13. Further, Figure 14 shows the balanced accuracies for the period 2 predictions across all datasets, again indicating how most models struggle distinguishing periodic snapshots.

**Homophily.** Table 8 shows the share of the top- $k$  edges that belong to intra-group and inter-group edges. Overall, these plots also illustrate how most models are able to distinguish between inter-group links and intra-group links, generally completely placing the minority edge group(s) at the bottom of these rankings. While the group-wise shares of edges among the top  $k$  edges are sometimes unbalanced in the homophilic SBM, these are often only due to slight differences in average edge probabilities, cf. Table 3.

**Preferential Attachment.** Figure 15 includes results for a denser graph with 4000 edges per timestep rather than the 2000 edges used in the main results. As for the sparser networks presented in Figure 6, we observe that across all models, predicted edge probabilities increase with the degree of the adjacent nodes.

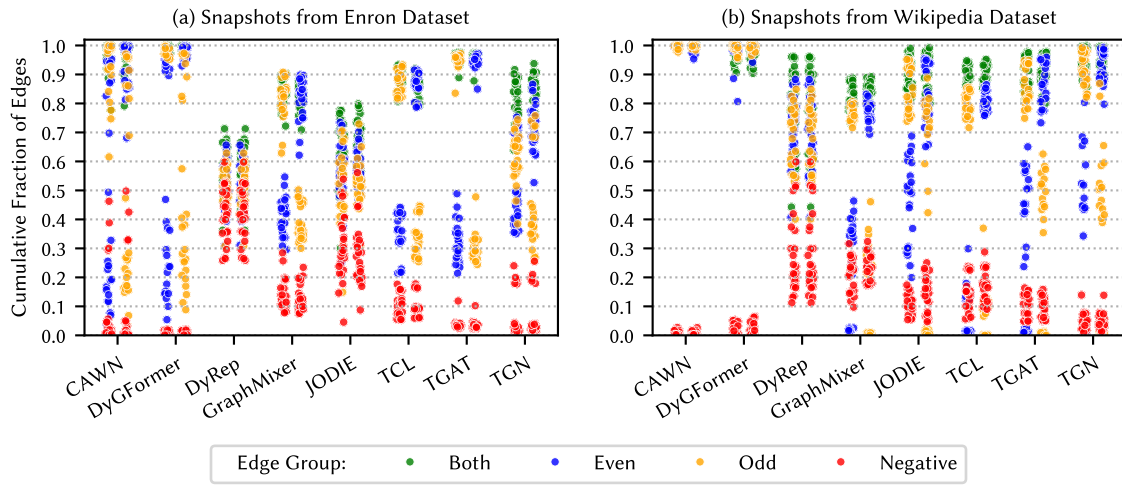


Figure 11: **Periodicity:** *ability of models to learn periodically repeated edges.* Additional results using snapshots from the Enron and Wikipedia datasets. Only *TGAT*, *TCL* and *GraphMixer* appear to consistently reproduce the periodic pattern.

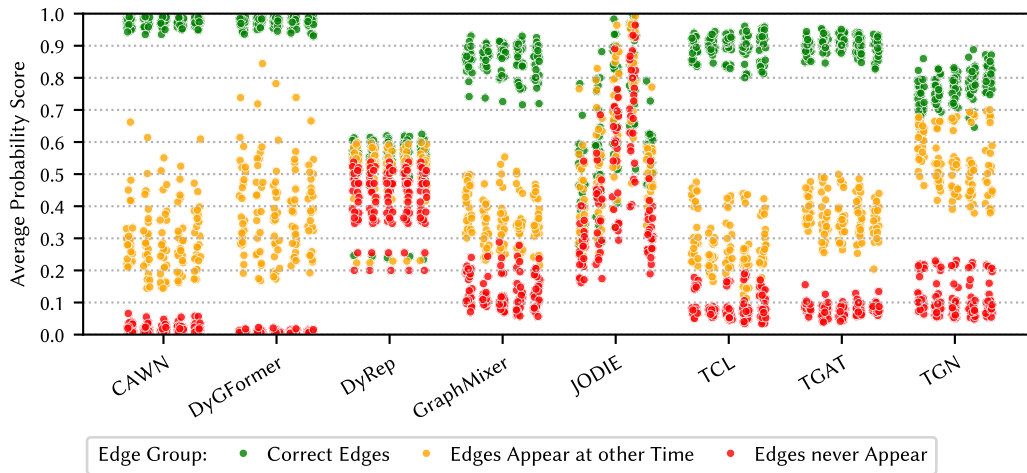


Figure 12: **Periodicity:** *ability of models to learn periodically repeated edges.* Additional results using snapshots from Enron with period 5. For each of the five timesteps, edges are grouped by whether they are (i) positive edges at this timestep, (ii) negative edges here, but positive at one or more other timesteps, or (iii) negative at all timesteps. Only *TGAT*, *TCL* and *GraphMixer* appear to consistently reproduce the periodic pattern. *CAWN*, *DyGFormer* and *TGN* do not sufficiently distinguish between edges for this timestep and those which appear at other timesteps.

## What Do Temporal Graph Learning Models Learn?

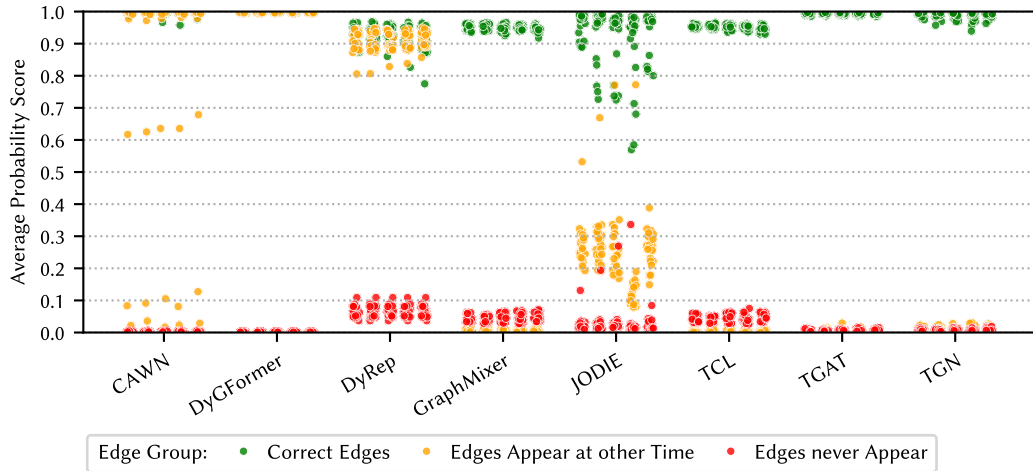


Figure 13: **Periodicity**: ability of models to learn periodically repeated edges. Additional results using snapshots from Wikipedia with period 5. For each of the five timesteps, edges are grouped by whether they are (i) positive edges at this timestep, (ii) negative edges here, but positive at one or more other timesteps, or (iii) negative at all timesteps. Only TGAT, TCL, GraphMixer and TGN appear to consistently reproduce the periodic pattern.

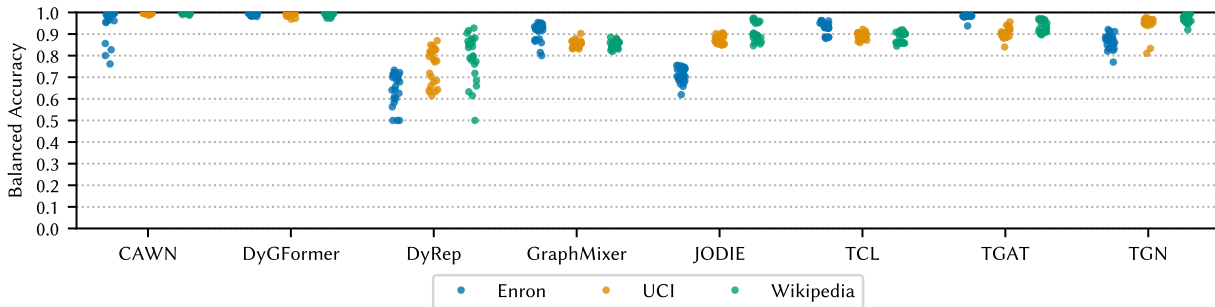


Figure 14: **Periodicity**: ability of models to learn periodically changing edges. We show the balanced accuracies of all models across all datasets and training seeds, with averages across odd and even test timesteps. CAWN, DyGFormer, GraphMixer, TCL TGAT and TGN appear to perform consistently well at this seemingly simple task. However, CAWN, DyGFormer, TGAT, and TGN also struggle to distinguish between edges appearing only at odd or even timesteps, cf. Figures 4 and 11.

Table 8: **Homophily**: ability of models to reproduce homophily in edge formation. We train graph learning models on stochastic block models with two groups (0 and 1), with intra-group being five times more likely than inter-group links (homophilic) or the reverse (heterophilic). We depict the ratio of the resulting edge groups among the top  $k$  most likely edges. Models generally prefer homophilic edges over heterophilic edges when trained on the homophilic data, and the reverse when trained on heterophilic data.

Edge Group	Homophilic SBM									Heterophilic SBM								
	Share within Top 1000 Edges			Share within Top 10,000 Edges			Share within Top 100,000 Edges			Share within Top 1000 Edges			Share within Top 10,000 Edges			Share within Top 100,000 Edges		
	0-0	0-1	1-1	0-0	0-1	1-1	0-0	0-1	1-1	0-0	0-1	1-1	0-0	0-1	1-1	0-0	0-1	1-1
<b>CAWN</b>	0.16	0.00	0.84	0.18	0.00	0.82	0.18	0.00	0.82	0.00	1.00	0.00	0.00	1.00	0.00	0.00	1.00	0.00
<b>DyGFormer</b>	0.44	0.00	0.56	0.40	0.00	0.60	0.45	0.00	0.55	0.00	1.00	0.00	0.00	1.00	0.00	0.00	1.00	0.00
<b>DyRep</b>	0.27	0.00	0.73	0.40	0.00	0.60	0.63	0.01	0.37	0.00	1.00	0.00	0.00	1.00	0.00	0.00	1.00	0.00
<b>GraphMixer</b>	0.20	0.00	0.80	0.26	0.00	0.74	0.34	0.00	0.67	0.00	1.00	0.00	0.00	1.00	0.00	0.00	1.00	0.00
<b>JODIE</b>	1.00	0.00	0.00	1.00	0.00	0.00	0.96	0.00	0.04	0.03	0.97	0.00	0.01	0.99	0.00	0.10	0.90	0.00
<b>TCL</b>	0.43	0.00	0.57	0.41	0.00	0.59	0.44	0.00	0.56	0.00	1.00	0.00	0.00	1.00	0.00	0.00	1.00	0.00
<b>TGAT</b>	0.20	0.00	0.80	0.16	0.00	0.84	0.18	0.00	0.82	0.00	1.00	0.00	0.00	1.00	0.00	0.00	1.00	0.00
<b>TGN</b>	0.39	0.00	0.61	0.68	0.03	0.29	0.41	0.41	0.17	0.00	1.00	0.00	0.08	0.91	0.01	0.68	0.26	0.07

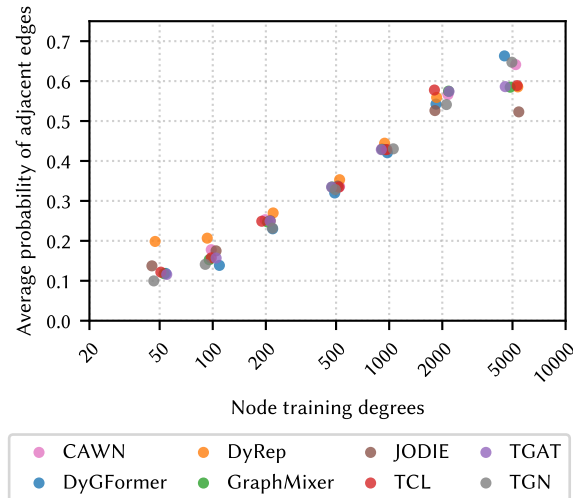


Figure 15: **Preferential Attachment:** *ability of models to reproduce preferential attachment in edge formation.* Additional results on denser BA graphs. While minimum degree is naturally higher, we observe a pattern consistent with the more shallow graphs: edge probabilities increase with degree of its adjacent nodes.

## C Results with Alternative Hyperparameters

Experiments have already explored the hyperparameter spaces for these models for a range of empirical datasets [28]. As such, we focus our resources on the synthetic data. Nevertheless, given the number of different datasets, seeds and models, extensive experimentation is costly. For hyperparameter tuning, we restricted the generation and training seeds to three variants rather than five.

Following Yu et al. [28], for *JODIE* we vary the dropout at intervals of 0.1 from 0.0 to 0.6, resulting in 99 additional models trained. For *TCL*, we switch to using uniform neighbor sampling and vary dropout at intervals of 0.2 from 0.0 to 0.6 (with fewer variants than *JODIE* due to the larger overall search space).

For persistence, Figure 16 shows the changes in dropout value have very little effect on the predictions from *JODIE*. With higher values of dropout, it can be seen in Figure 17a that *TCL* stops distinguishing between the two groups of edges, whilst uniform neighbor sampling completely degrades performance. The same effects are observed for periodicity in Figures 17b and 18. The recency results for *JODIE*, *TCL*, and *TGN* do not change with variations of hyperparameters, as shown in Figures 19, 20 and 21.

# What Do Temporal Graph Learning Models Learn?

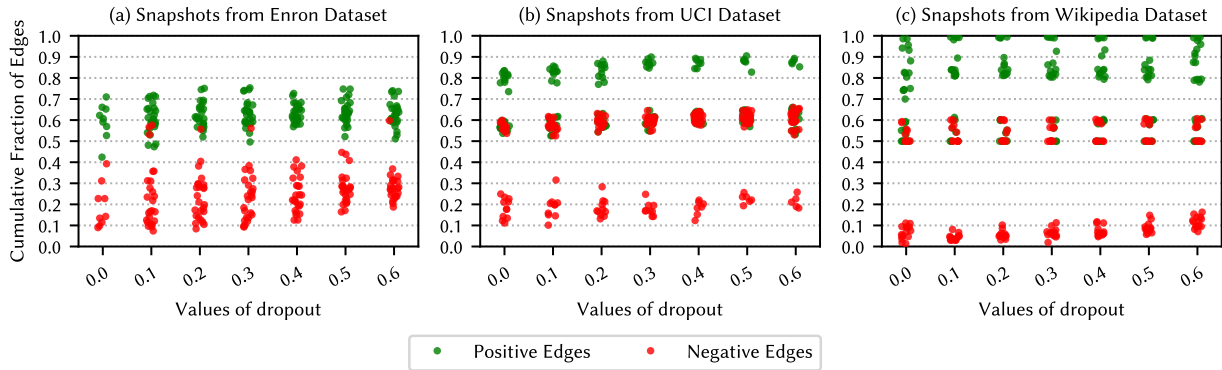
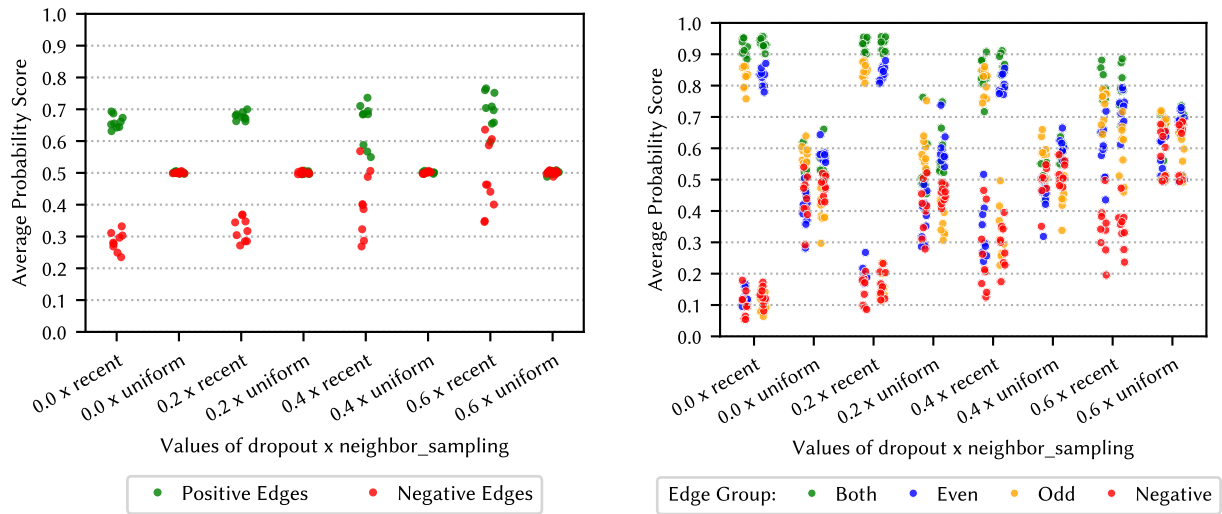


Figure 16: **Persistence**: results for different hyperparameters for JODIE.



(a) Persistence: results on UCI.

(b) Periodicity: results on UCI.

Figure 17: Impact of hyperparameters for TCL.

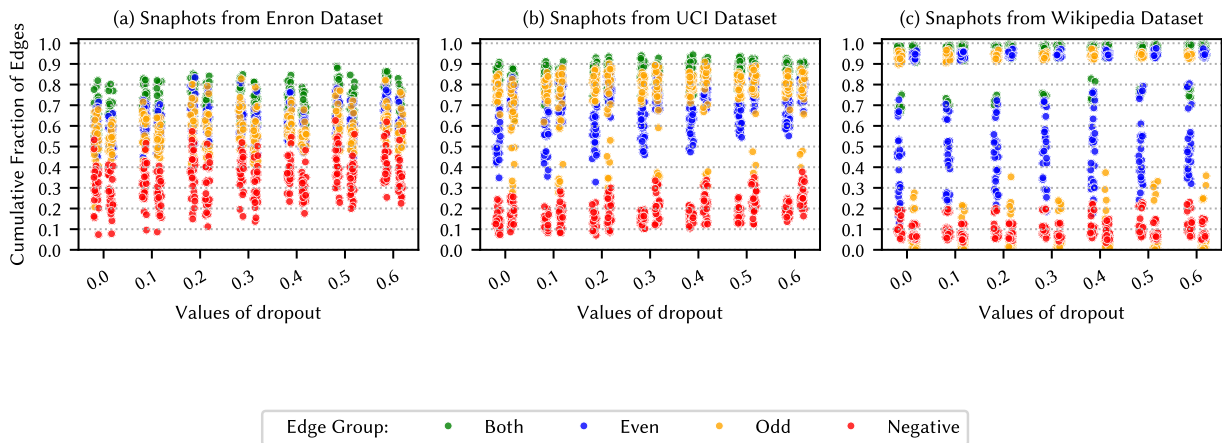


Figure 18: **Periodicity**: results for different hyperparameters for JODIE.

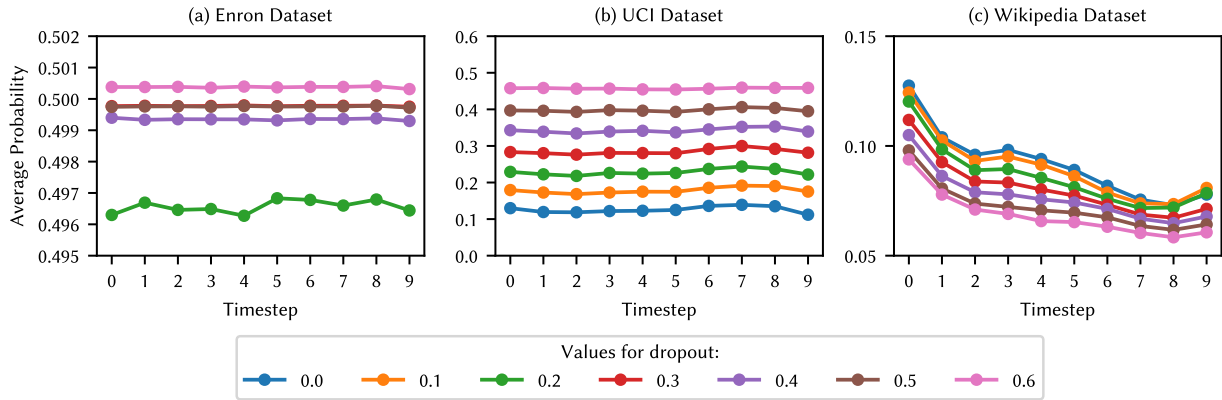


Figure 19: **Recency**: results for different hyperparameters for JODIE.

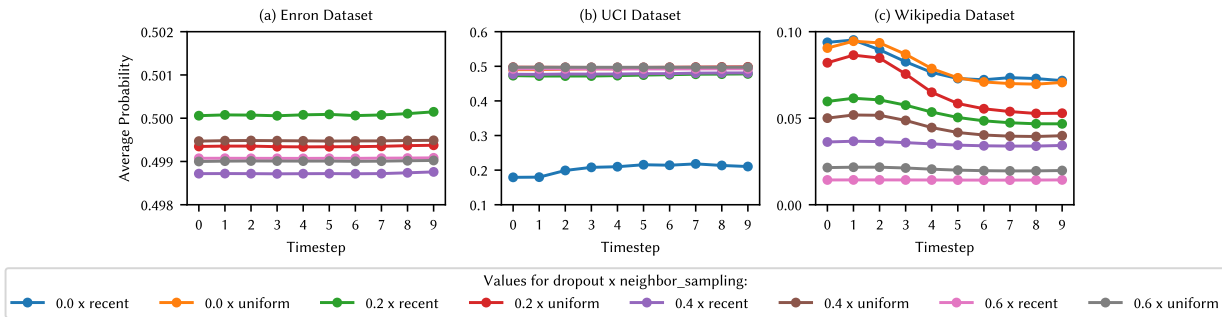


Figure 20: **Recency**: results for different hyperparameters for TCL.

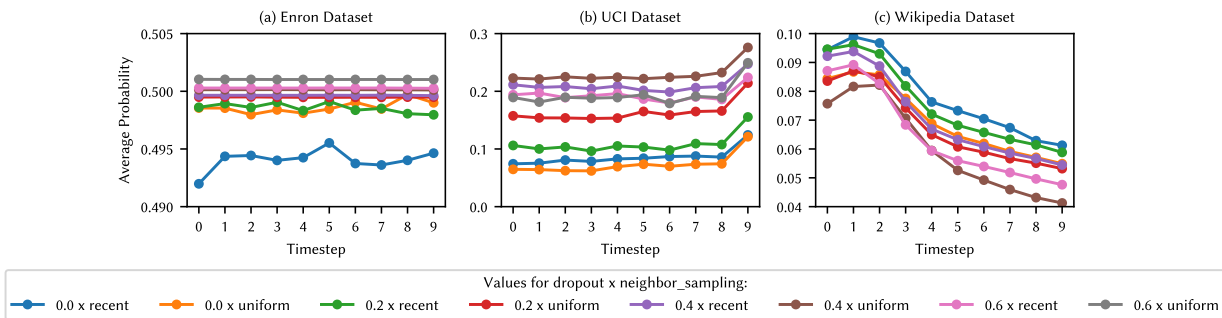


Figure 21: **Recency**: results for different hyperparameters for TGN.